Compressive Imaging and Resolution

Albert Fannjiang

University of California, Davis, CA, USA

CoSeRa 2016, Aachen, Germany
September 21, 2016

Outline

- Two imaging geometries: paraxial and scattering.
- Theoretical benchmarks
- Subspace methods: MUSIC, ESPRIT.
- General CS techniques with unresolved grids.
- Coherence bounds for SIMO
- Nonlinear inversion with multiple-shot SIMO
- Extended targets.
- Conclusion

Fundamental equations

Helmholtz equation: monochromatic wave u

$$\Delta u(\mathbf{r}) + \omega^2(1+\nu(\mathbf{r}))u(\mathbf{r}) = 0, \quad \mathbf{r} \in \mathbb{R}^d, \quad d = 2, 3$$

where ν describes the medium heterogeneities.
Data: the scattered field $u^{\mathrm{s}} = u - u^{\mathrm{i}}$ governed by

$$\Delta u^{\mathrm{s}} + \omega^2 u^{\mathrm{s}} = -\omega^2 \nu u.$$

Lippmann-Schwinger integral equation:

$$u^{\mathrm{s}}(\mathbf{r}) \;\; = \;\; \omega^2 \int \nu(\mathbf{r}') \left(u^{\mathrm{i}}(\mathbf{r}') + u^{\mathrm{s}}(\mathbf{r}') \right) G(\mathbf{r}, \mathbf{r}') d\mathbf{r}'$$

where

$$G(\mathbf{r}, \mathbf{r}') = \begin{cases} \frac{e^{i\omega|\mathbf{r}-\mathbf{r}'|}}{4\pi|\mathbf{r}-\mathbf{r}'|}, & d = 3 \\ \frac{i}{4} H_0^{(1)}(\omega|\mathbf{r}-\mathbf{r}'|), & d = 2. \end{cases}$$

Imaging geometry

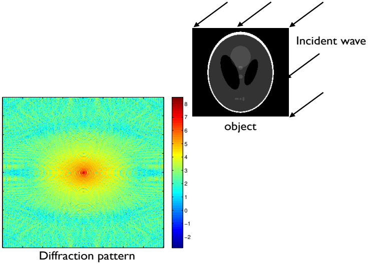

(a) Full view: paraxial

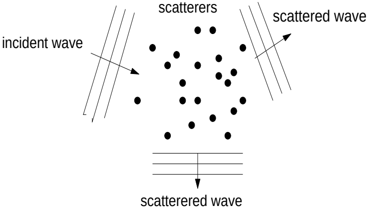

(b) Side view: scattering

- **Paraxial geometry**: With $\mathbf{r} = (\mathbf{x}, z_0), \mathbf{r}' = (\mathbf{x}', 0)$, we have

$$G(\mathbf{x}, \mathbf{x}') = C e^{i\omega|\mathbf{x}|^2/(2z_0)} e^{-i\omega \mathbf{x}\cdot\mathbf{x}'/z_0} e^{i\omega|\mathbf{x}'|^2/(2z_0)}$$

$$u^{\mathrm{s}}(\mathbf{r}) = \omega^2 e^{i\omega|\mathbf{x}|^2/(2z_0)} \int \underbrace{\nu(\mathbf{r}')u(\mathbf{r}')e^{i\omega|\mathbf{x}'|^2/(2z_0)}}_{\text{masked object}} \overbrace{e^{-i\omega \mathbf{x}\cdot\mathbf{x}'/z_0}}^{\text{Fourier}} d\mathbf{r}'$$

- **Scattering geometry:** incident direction $\hat{\mathbf{d}}$

$$u^{\mathrm{s}}(\mathbf{r}) = \frac{e^{i\omega|\mathbf{r}|}}{|\mathbf{r}|^{(d-1)/2}} \left(A(\hat{\mathbf{r}}, \hat{\mathbf{d}}) + \mathcal{O}\left(\frac{1}{|\mathbf{r}|}\right)\right), \quad \hat{\mathbf{r}} = \frac{\mathbf{r}}{|\mathbf{r}|}$$

where A is the scattering amplitude

$$A(\hat{\mathbf{r}}, \hat{\mathbf{d}}) \;=\; \frac{\omega^2}{4\pi} \int_{\mathbb{R}^d} \underbrace{\nu(\mathbf{r}') \left(u^{\mathrm{i}}(\mathbf{r}') + u^{\mathrm{s}}(\mathbf{r}')\right)}_{\text{masked object}} \overbrace{e^{-i\omega \mathbf{r}' \cdot \hat{\mathbf{r}}}}^{\text{deficient}} \, d\mathbf{r}'.$$

- Nonlinear inversion.
- Born approximation: drop u^{s}.

Point objects and sensors

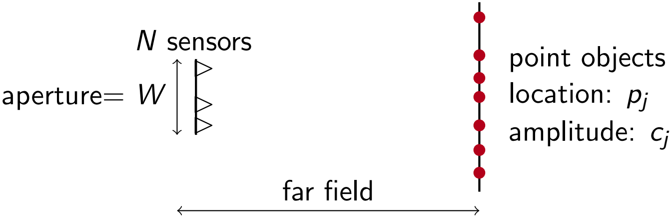

- Point objects located at $p_j \in [0,1], j = 1, ..., s$.
- Signal received at $q_k \in [0, W], k = 1, \ldots, N$

$$y_k = \underbrace{\sum_{j=1}^{s} c_j e^{-2\pi i q_k p_j}}_{\text{signal received by the } k\text{th sensor}} + \underbrace{e_k}_{\text{measurement noise}} .$$

- Resolution Length (RL) $=$ (Aperture)$^{-1} = 1/W$: Sidelobes of two points (Abbe 1873, Rayleigh 1879)

Discrete signal model: $y = \Phi x + e$

- Discretization of the continuum system: replace p_j by the closest point in $\{m/M : m = 0, \ldots, M-1\}$.

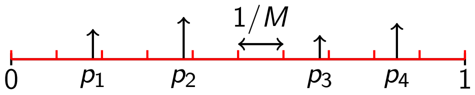

- Set $x_m = c_j$ if m/M is the closest point to some p_j and zero otherwise.
- Sensing matrix $\Phi \in \mathbb{C}^{N \times M}$ with $\Phi_{k,m} = e^{-2\pi i q_k m/M}$.
- $e =$ measurement noise $+$gridding (model) error
- Sampling theorem for unit-bandlimited, M-periodic signals:
  1. The discrete samples at $q_k = 0, .., M-1$ uniquely determine the signal.
  2. With noise/error, continuum sampling is not equivalent to Nyquist sampling.

Resolution

1. Minimum separation
2. Noise stability
3. Number of objects
4. Number of measurement data
5. Computational complexity
6. Flexibility of measurement schemes
7. etc...

Resolution of optimal recovery (Donoho 1992)

- Minimax error

$$E = \inf_{\tilde{x}} \sup_{x} \|\tilde{x} - x\|, \quad \text{s.t. } \|\Phi x - \Phi \tilde{x}\| < \epsilon.$$

- No concrete algorithm.
- Full continuum Fourier measurement: $t \in [0, W]$.
- Fine grid spacing $1/F$ RL where $F = \#$ grid points per RL (the refinement factor).
- Spike train but sparsity not explicit.
- Uniqueness requires minimum separation > 2 RL.
- Stability if minimum separation ≥ 4 RL.
- Demanet & Nguyen 2015: For $\|x\|_0 = s$ with minimum separation = grid spacing $1/F$ RL

$$E \sim \epsilon F^{2s-1}$$

Gridless L1-minimization

- Candès & Fernandez-Granda 2013, 2014:

$$\min \|\tilde{x} - x\|_1, \quad \|y - \Phi x\|_1 < \epsilon$$

  1. Minimum separation ≥ 4 RL
  2. Full continuum Fourier measurement
  3. Sparsity not explicit.
  4. Stability: $\|\tilde{x} - x\|_1 \leq c\epsilon F^2$.

- Tang, Bhaskar, Shah & Recht 2013
  1. Minimum separation ≥ 4 RL.
  2. Noiseless data $\epsilon = 0$.
  3. $\mathcal{O}(s)$ partial Fourier measurement.
  4. Uniqueness of L1-minimization.

Single-snapshot MUSIC (Schmidt 1981)

- Full discrete measurement: $q_k = (k-1), k = 1, ..., N$
- Hankel matrix

$$
\begin{aligned}
H &= \begin{bmatrix} y_1 & y_2 & \cdots & y_{N-L+1} \\ y_2 & y_3 & \cdots & y_{N-L+2} \\ \vdots & \vdots & \vdots & \vdots \\ y_L & y_{L+1} & \cdots & y_N \end{bmatrix} = \Phi^L X (\Phi^{N-L})^T \\
X &= \mathrm{diag}(x_1, \ldots, x_s)
\end{aligned}
$$

with Vandermonde matrix

$$
\Phi^L = \begin{bmatrix} 1 & 1 & \cdots & 1 \\ e^{-2\pi i p_1} & e^{-2\pi i p_2} & \cdots & e^{-2\pi i p_s} \\ (e^{-2\pi i p_1})^2 & (e^{-2\pi i p_2})^2 & \cdots & (e^{-2\pi i p_s})^2 \\ \vdots & \vdots & \vdots & \vdots \\ (e^{-2\pi i p_1})^{L-1} & (e^{-2\pi i p_2})^{L-1} & \cdots & (e^{-2\pi i p_s})^{L-1} \end{bmatrix}.
$$

- With $L \geq s+1$ and $N - L + 1 \geq s$, $\mathrm{Ran}\{H\} = \mathrm{Ran}\{\Phi^L\}$ are a proper subspace (the signal space) of $\mathbb{C}^L$.

MUSIC (continued)

- Noise subspace = Orthogonal complement of the signal space.
- $\tilde{S}$ = the peaks of $J(p) = (\mathcal{P}\phi^L(p))^{-1}$,
  $\mathcal{P}$ = projection onto the noise space.
- SVD to identify the signal and noise subspaces.
- Perfect recovery with noiseless data $N \geq 2s$ and without minimum separation constraint.
- Stability of support recovery with minimum separation > 2 RL by MUSIC (Liao & F. 2016) and ESPRIT (F. 2015).

Discrete Ingham inequality

Control the largest and least singular values

Theorem

If S satisfies the separation condition

$$\delta = \min_{j \neq l} d(p_j, p_l) > \frac{1}{L}\Big(1 - \frac{2\pi}{L}\Big)^{-\frac{1}{2}}$$

then

$$\frac{\|\Phi^L z\|_2^2}{\|z\|_2^2} \geq L\Big(\frac{2}{\pi} - \frac{2}{\pi L^2 \delta^2} - \frac{4}{L}\Big).$$

and

$$\frac{\|\Phi^L z\|_2^2}{\|z\|_2^2} \leq L\Big(\frac{4\sqrt{2}}{\pi} + \frac{\sqrt{2}}{\pi L^2 \delta^2} + \frac{3\sqrt{2}}{L}\Big)$$

Noise stability

Corollary

For $L = \left[\frac{N+1}{2}\right]$ *and the separation condition*

$$\delta > \frac{2}{N}\left(1 - \frac{4\pi}{N}\right)^{-\frac{1}{2}} = \left(1 - \frac{4\pi}{N}\right)^{-\frac{1}{2}} 2\mathrm{RL}$$

the singular values of H *satisfy*

$$\begin{aligned} \sigma_1 &\leq c_1 N x_{\max} \\ \sigma_s &\geq c_2 N x_{\min} \end{aligned}$$

where $c_1 \leq 3c_2$.

Condition number of $H \leq 3x_{\max}/x_{\min}$
if the minimum separation is slightly greater than 2 RL

Gridless recovery by MUSIC/ESPRIT

Reconstruction of 15 objects separated by 3-4 RL with 10% NSR.

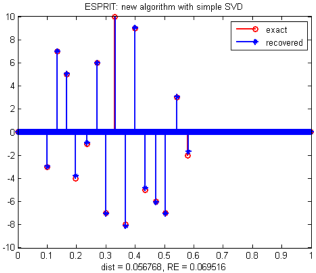

(a) ESPRIT: $\mu_{\mathrm{H}}(\tilde{S}, S) = 0.057$RL

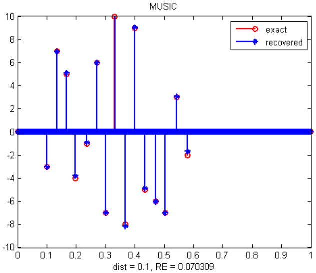

(b) MUSIC: $\mu_{\mathrm{H}}(\tilde{S}, S) = 0.1$RL.

Hausdorff metric of support error is often a small fraction of 1 RL

MUSIC/ESPRIT: object separation of 2-3 RL

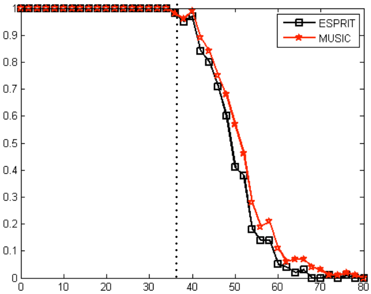

(a) Success rate versus NSR

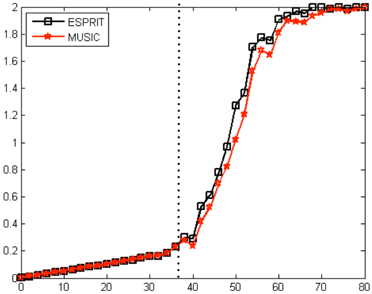

(b) Average HM (in the unit of RL) versus NSR

Success if Hausdorff metric is less than 1 RL. Significant error can be tolerated by MUSIC/ESPRIT,

Superresolution: separation < 1 RL with noisy data

Log-relative error vs. NSR and separation

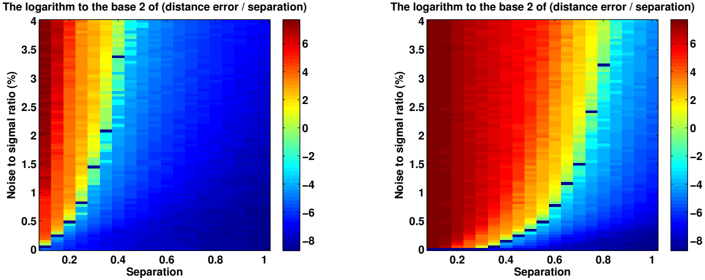

(a) Two-point resolution

(b) Three-point resolution

- Recall: Noise $\sim$ (minimum separation)$^{2s-1}$ (Demanet & Nguyen 2015)
- MUSIC: empirical power law with the following exponents

$$e(2) = 3.6, \quad e(3) = 6, \quad e(4) = 8.4, \quad e(5) = 11$$

which are slightly greater than $2s - 1$.

Gridless compressed sensing

1. Gridless or unresolved fine grids.
2. Sparse measurement under sparsity constraint.
3. Versatility: random, non-Fourier measurements.
4. Noise Stability.
5. Resolution.

Gridding error vs mutual coherence

- Refinement factor
$$F = \frac{1 \text{ RL}}{\text{grid spacing}} = \#\text{ grid points per 1 RL}$$
- Pairwise coherence: the normalized scalar product of $(e^{-2\pi i q_k x_1})_{k=1}^N$ and $(e^{-2\pi i q_k x_2})_{k=1}^N$.

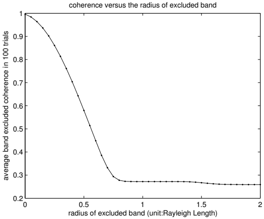

(a) Average pairwise coherence versus $|x_1 - x_2|$

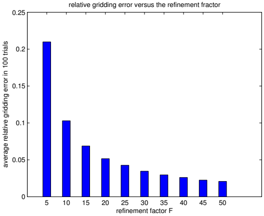

(b) Gridding error

- Relative griding error inversely proportional to F.
- Mutual coherence $\mu \approx 0.996$ for $F = 20$.

CS with $F = 1$

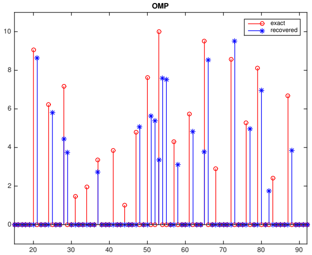

(a) OMP

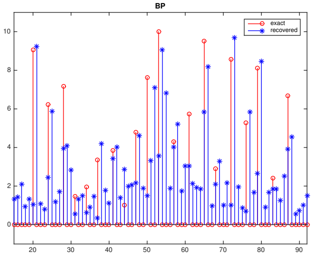

(b) L1-min

minimum separation ≥ 3 RL, noise-free

CS with $F = 50$

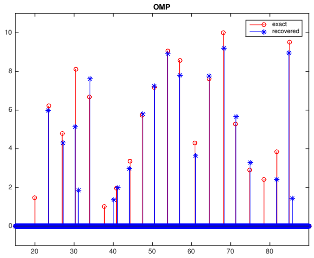

(a) OMP

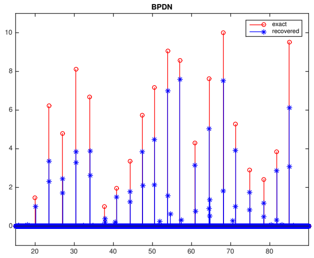

(b) L1-min

minimum separation $\geq$ 3 RL, SNR $= 20$

Post-processing of L1-min

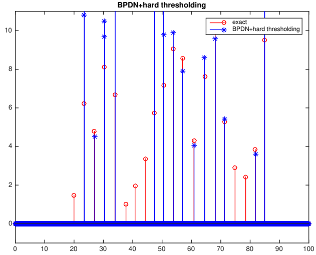

(a) hard thresholding

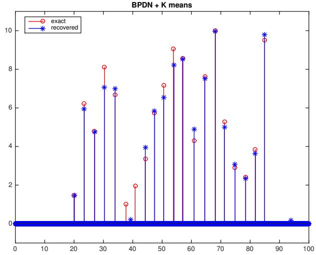

(b) K-mean

MUSIC with joint sparsity CS (F. 2011)

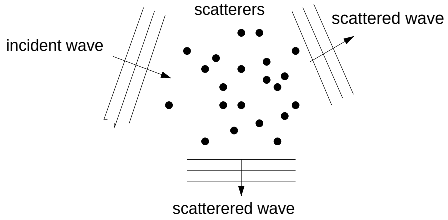

- General form: $Y = \Phi X \Psi^*$.
- Φ: re-propagation matrix
- Ψ: columns represent different illuminations.
- CS with joint sparsity.

CS MUSIC (continued)

- Support-indexed RIP: for all z supported on the set S

$$(1-\delta_S^-)\|z\|_2^2 \le \|\Phi z\|_2^2 \le (1+\delta_S^+)\|z\|_2^2$$

- For any set $K, |K| \le k$, we have the trivial bound

$$\delta_K^\pm \le (k-1)\mu(\Phi_K).$$

- For ℓ = tolerance of support error and S_ℓ=ℓ-neighborhood of S. define

$$\delta_{S'}^\pm = \sup_{p\notin S_\ell} \delta_{S\cup\{p\}}^\pm.$$

- $\delta_S^\pm, \delta_{S'}^\pm$ determine the noise stability of support recovery of accuracy ℓ.

CS MUSIC (continued)

Theorem (F. 2011)

For some explicitly defined algebraic functions f and g,

$$\frac{\epsilon}{x_{\min}} < g\left(\frac{x_{\max}}{x_{\min}}, \delta_S^{\pm}, \delta_{S'}^{\pm}\right)$$

implies the thresholding rule Θ is accurate up to ℓ:

$$S \subseteq \Theta := \left\{J > f\left(\frac{\epsilon}{x_{\min}}\right)\right\} \subseteq S_\ell.$$

- Minimum separation $> 2\ell = \mathcal{O}(1)$ RL $\Longrightarrow$ stability.
- $\mathcal{O}(s^2)$ noisy incoherent measurement
- Advantages: simple, versatility, stability, resolution.
- Disadvantages: Need (s times) more data than CS theory.

Coherence band

Coherence band: Let $\eta \in (0,1)$. Define the η-coherence band of Column k to be the set

$$B_\eta(k) = \{i \mid \mu(i,k) > \eta\},$$

and the η-coherence band of the column set S to be the set

$$B_\eta(S) = \cup_{k \in S} B_\eta(k).$$

Double coherence band:

$$B_\eta^{(2)}(k) := B_\eta(B_\eta(k)) = \cup_{j \in B_\eta(k)} B_\eta(j)$$
$$B_\eta^{(2)}(S) := B_\eta(B_\eta(S)) = \cup_{k \in S} B_\eta^{(2)}(k)$$

Coherence band

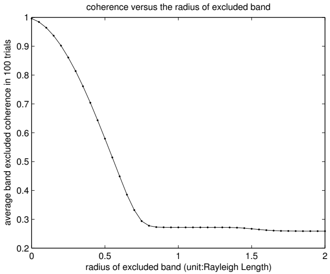

Radius of $B_\eta \leq 1$ RL

Localized coherence band has a simple physical interpretation.

Technique I: Band exclusion

Idea: exclude the double coherence band of recovered objects

Example:

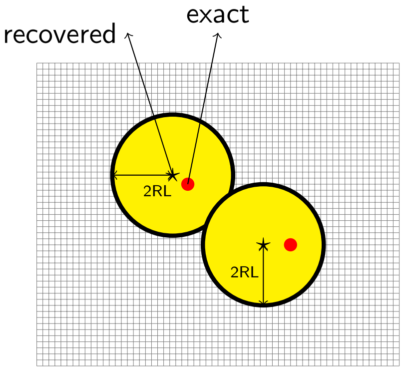

Band-excluding OMP (BOMP)

Algorithm 1. BOMP

Input: $\Phi, y, s, \eta > 0$
Initialization: $x^0 = 0, r^0 = y$ and $S^0 = \emptyset$
Iteration: For $n = 1, ..., s$

1) $i_{\max} = \arg\max_i |\langle r^{n-1}, \Phi(:, i)\rangle|, i \notin B_\eta^{(2)}(S^{n-1})$
2) $S^n = S^{n-1} \cup \{i_{\max}\}$
3) $x^n = \arg\min_z \|\Phi z - y\|_2$ s.t. $\mathrm{supp}(z) \in S^n$
4) $r^n = y - \Phi x^n$

Output: x^s.

Theorem (F. & Liao 2012)

Let x be s-sparse and $\eta > 0$ be fixed. Suppose that

$$B_\eta(i) \cap B_\eta^{(2)}(j) = \emptyset, \quad \forall i, j \in supp(x),$$
$$\eta(5s-4)\frac{x_{\max}}{x_{\min}} + \frac{5\|e\|_2}{2x_{\min}} < 1$$

where $x_{\max} = \max_k |x_k|$, $\quad x_{\min} = \min_k |x_k|$. Let $\tilde{x}$ be the BOMP reconstruction. Then every nonzero component of $\tilde{x}$ is in the η-coherence band of a unique nonzero component of x.

- compression $N \sim s^2 x_{\max}^2 / x_{\min}^2$.
- minimum separation ≤ 3 RL
- support accuracy ≤ 1 RL

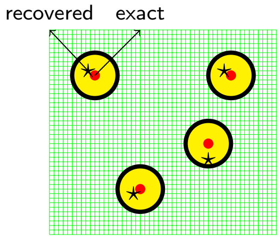

Technique II: Local optimization (LO)

Algorithm 2. Local Optimization (LO)

Input: $\Phi, y, \eta > 0, S^0 = \{i_1, \dots, i_k\}$

Iteration: For $n = 1, 2, ..., k$

1) $x^n = \arg\ \min_z \|\Phi z - y\|_2$
   $\mathrm{supp}(z) = (S^{n-1} \backslash \{i_n\}) \cup \{j_n\},\ j_n \in B_\eta(\{i_n\})$
2) $S^n = \mathrm{supp}(x^n)$

Output: S^k

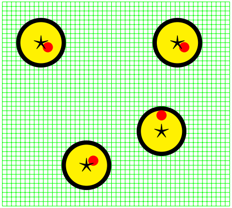

- Residual reduction
- Efficient, local computation
- Performance guarantee: does not ruin the support recovery.

Locally Optimized BOMP (BLOOMP)

Algorithm 3. BLOOMP

Input: $\Phi, y, s, \eta > 0$

Initialization: $x^0 = 0, r^0 = y$ and $S^0 = \emptyset$

Iteration: For $n = 1, ..., s$

1) $i_{\max} = \arg\max_i |\langle r^{n-1}, a_i \rangle|, i \notin B_\eta^{(2)}(S^{n-1})$
2) $S^n = \mathrm{LO}(S^{n-1} \cup \{i_{\max}\})$
3) $x^n = \arg\min_z \|\Phi z - y\|_2$ s.t. $\mathrm{supp}(z) \in S^n$
4) $r^n = y - \Phi x^n$

Output: x^s.

CS with BLO: F=50, SNR = 20

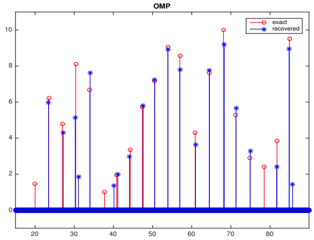

(a) OMP

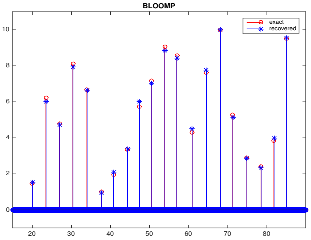

(b) BLOOMP

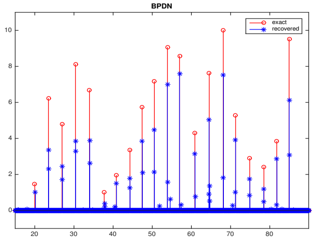

(c) BP

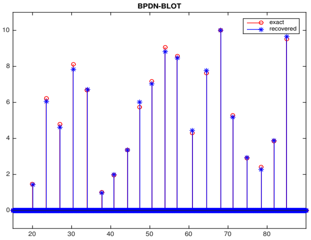

(d) BP-BLOT

BLO-based CS algorithms

- **Greedy**

  BLO Subspace Pursuit
  BLO CoSaMP
  BLO Iterative Hard Thresholding

- **L1-min**

BP-BLOT	constrained L_1 minimization
Lasso-BLOT	L_1 regularization

- BLOOMP outperforms in noise stability and dynamic range.
- L1-BLOT outperforms in sparsity of measurement (no proof).

Performamce comparison with sparse measurement

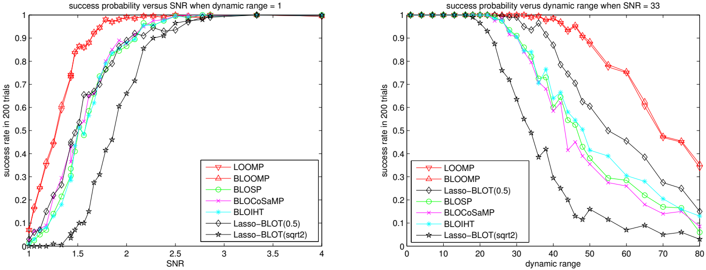

Figure: Success probability versus (left) SNR for dynamic range 1 and (right) dynamic range for SNR $= 33$.

Performance comparison with full discrete/continuum Fourier measurement

Objects separated between 4 RL and 5 RL.

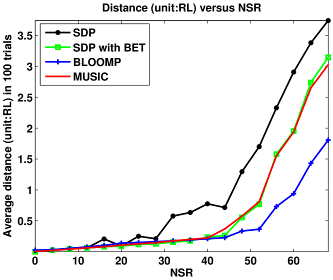

(a) Dynamic range = 1. Average running time for SDP and MUSIC is 20.3583s and 0.3627s, respectively, while the average running time for BLOOMP is 6.3420s ($F = 20$).

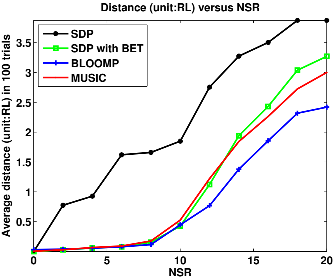

(b) Dynamic range = 10. Average running time for SDP and MUSIC is 20.5913s and 0.3661s, respectively, while the average running time for BLOOMP is 6.2623s ($F = 20$).

MUSIC outperforms BLOOMP when separation drops below 3 RL.

Resolution in scattering geometry

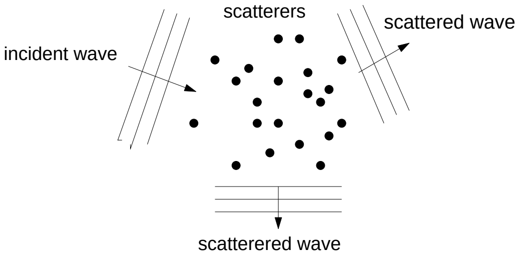

- Data: scattering amplitude

$$A(\hat{\mathbf{r}}, \hat{\mathbf{d}}) \;=\; \frac{\omega^2}{4\pi} \int_{\mathbb{R}^d} \overbrace{\nu(\mathbf{r}') \left(u^{\mathrm{i}}(\mathbf{r}') + u^{\mathrm{s}}(\mathbf{r}')\right)}^{\text{masked object}} \underbrace{e^{-i\omega \mathbf{r}' \cdot \hat{\mathbf{r}}}}_{\text{deficient}} d\mathbf{r}'$$

- Single frequency with $\hat{\mathbf{r}} \in \mathbb{S}^{d-1}$: deficient in dimension.
- Longitudinal resolution vs transverse resolution
- Shadowing

2D Single-Input-Multiple-Output (SIMO)

- SIMO: One transmission and N receptions $\Longrightarrow \{\hat{\mathbf{r}}_j\}$.
- Discretize the domain into a unresolvable fine grid $\{\mathbf{r}'_k\}$.
- $\Phi = [e^{-i\omega \mathbf{r}'_k \cdot \hat{\mathbf{r}}_j}]$: dimensionally deficient Fourier measurement.

Let $\ell \ll 1$ RL be the fine-grid spacing and f^{s} the density function of reception.

Theorem (F. 2010)

$$\mu_{\mathbf{p},\mathbf{q}} < \frac{c_1}{\sqrt{N}} + \frac{c_2 \sup_\theta \left\{ |f^{\mathrm{s}}(\theta)|, \left| \frac{d}{d\theta} f^{\mathrm{s}}(\theta) \right| \right\}}{\sqrt{1 + \omega\ell|\mathbf{p} - \mathbf{q}|}}$$

with high probability.

- Resolution $= \mathcal{O}(\omega^{-1})$; decay power $1/2$.
- Recall: $\eta(5s-4)\frac{x_{\max}}{x_{\min}} + \frac{5}{2}\frac{\epsilon}{x_{\min}} < 1$

3D SIMO

Theorem (F. 2010)

$$\mu_{\mathbf{p},\mathbf{q}} < \frac{c_1}{\sqrt{N}} + \frac{c_2 \sup_\theta \left\{ |f^{\mathrm{s}}(\theta)|, \left|\frac{d}{d\theta} f^{\mathrm{s}}(\theta)\right| \right\}}{1 + \omega\ell|\mathbf{p}-\mathbf{q}|}$$

with high probability.

- Resolution $= \mathcal{O}(\omega^{-1})$; decay power $=1$.
- Recall: $\eta(5s-4)\frac{x_{\max}}{x_{\min}} + \frac{5}{2}\frac{\epsilon}{x_{\min}} < 1$

Nonlinear inversion with point objects

- Masked object $\nu(\mathbf{r}')\left(u^{\mathrm{i}}(\mathbf{r}') + u^{\mathrm{s}}(\mathbf{r}')\right)$ shares the same support.
- Multiple shots: masked objects $\mathbf{F} = [\mathbf{f}_1, ..., \mathbf{f}_n]$ of joint sparsity

$$\mathbf{G} = \Phi\mathbf{F} + \mathbf{E}$$

where $\mathbf{G} = [\mathbf{g}_1, ..., \mathbf{g}_n]$ is the data vector and $\mathbf{E}$ represents noise.

BLOOMP with joint sparsity

Algorithm BLOOMP with joint sparsity

Input: $\Phi_1, ..., \Phi_n, \mathbf{G}, \eta > 0$

Initialization: $\mathbf{F}^0 = 0, \mathbf{R}^0 = \mathbf{G}$ and $S^0 = \emptyset$

Iteration: For $k = 1, ..., s$

1) $i_{\max} = \arg\max_i \sum_{j=1}^{J} |\Phi_{j,i}^{\dagger} \mathbf{r}_j^{k-1}|, i \notin B_\eta^{(2)}(S^{k-1})$.
2) $S^k = \mathrm{JLO}(S^{k-1} \cup \{i_{\max}\})$.
3) $[\mathbf{f}_1^k, ..., \mathbf{f}_n^k] = \arg\min_{\mathbf{H}} \|[\Phi_1 \mathbf{h}_1, ..., \Phi_n \mathbf{h}_n] - \mathbf{G}\|_{\mathrm{F}}$ s.t. $\cup_j \mathrm{supp}(\mathbf{h}_j) \subseteq S^k$
4) $[\mathbf{r}_1^k, ..., \mathbf{r}_n^k] = \mathbf{G} - [\Phi_1 \mathbf{f}_1^k, ..., \Phi_n \mathbf{f}_n^k]$

Output: $\mathbf{F}_* = [\mathbf{f}_1^s, ..., \mathbf{f}_n^s]$.

- Masked object $\Longrightarrow$ object:

$$\nu_* = \arg\min_{\mathbf{v}} \sum_{j=1}^{n} \|(\omega^2 \mathbf{\Gamma} \mathbf{f}_j^{\mathrm{s}} + \mathbf{u}_j^{\mathrm{i}})\mathbf{v} - \mathbf{f}_j^{\mathrm{s}}\|_2^2.$$

$$\text{where} \quad \mathbf{\Gamma} = [(1 - \delta_{jl}) G(\mathbf{r}_j, \mathbf{r}_l)]$$

Inverse Born scattering with Zernike basis (F. 2015)

- For $m \in \mathbb{Z}, n \in \mathbb{N}$, $n \geq |m|$ and $n - |m|$ even,

$$V_n^m(x,y) = R_n^m(\rho)e^{im\theta}, \quad x^2 + y^2 \leq 1$$

where

$$R_n^m(\rho) \;=\; \frac{1}{(\frac{n-|m|}{2})\rho^{|m|}} \left[\frac{d}{d(\rho^2)}\right]^{\frac{n-|m|}{2}} \left[(\rho^2)^{\frac{n+|m|}{2}}(\rho^2-1)^{\frac{n-|m|}{2}}\right]$$

are n-th degree Zernike polynimials, $R_n^m(1) = 1$ for all permissible values of m, n.

- Sparser than Bessel-Fourier or Chebyshev-Fourier expansion (Boyd and Yu 2011, Boyd and Petschek 2014).
- Born approximation with plane-wave incidence: $\mathbf{s} = \hat{\mathbf{r}} - \hat{\mathbf{d}}$.

  Resolution $= \mathcal{O}(\omega^{-1})$; decay power $= 1$

.

Conclusion

- Compressive imaging in the continuum.
- Resolution w.r.t. noise, number/complexity of objects and measurement data.
- Versatility of reconstruction schemes w.r.t. measurement schemes: MUSIC, BLO-based techniques etc.
- Point vs. extended objects.
- Multiple vs. Born scattering.

References

1. D. L. Donoho, "Superresolution via sparsity constraints", *SIAM J. Math Anal* **23** (1992): 1309-1331.
2. E. J. Candès & C. Fernandez-Granda,"Super-resolution from noisy data" , *J. Fourier Anal. Appl.* **19(6)** (2013): 1229-1254.
3. E.J. Candès & C. Fernandez-Granda, "Towards a mathematical theory of super-resolution," *Commun. Pure Appl. Math.* **67(6)** (2014): 906-956.
4. L. Demanet & N. Nguyen, "The recoverability limit for superresolution via sparsity," arXiv:1502.01385.
5. A. Fannjiang, "Compressive inverse scattering I. High frequency SIMO/MISO and MIMO measurements, " *Inverse Probl.* **26** (2010): 035008.
6. A. Fannjiang, "The MUSIC algorithm for sparse objects: a compressed sensing analysis", *Inverse Problems* **27** (2011): 035013.
7. A. Fannjiang, "Compressive Sensing Theory for Optical Systems Described by a Continuous Model," in *Optical Compressive Imaging*, arXiv:1507.00794.
8. A. Fannjiang & W. Liao, "Coherence pattern-guided compressive sensing with unresolved grids", *SIAM Journal on Imaging Science* **5** (2012):179-202.
9. W. Liao & A. Fannjiang, "MUSIC for single-snapshot spectral estimation: Stability and super-resolution," *Appl. Comput. Harm. Anal.* **40** (2016): 33-67.
10. G. Tang, B. Bhaskar, P. Shah & B. Recht, "Compressed sensing off the grid", *IEEE Transactions on Information Theory* **59** (2013): 7465-7490.

THANK YOU!